

## GAM-7: An Organic-Inorganic Hybrid Layered Aluminophosphate Crystal Formed by Zeolite Transformation

Kenichi Komura,<sup>1,2\*</sup> Gensuke Nakai,<sup>1</sup> Soki Shimizu,<sup>2</sup> Matsuri Nomura,<sup>1</sup> Shiori Niwa,<sup>2</sup> Sanae Kagari,<sup>1</sup> Kazuma Oka,<sup>1</sup> Edo Imai,<sup>1</sup> Hisakazu Aoki,<sup>1</sup> and Takuji Ikeda<sup>3\*</sup>

<sup>1</sup> Department of Materials Science and Processing, Graduated School of Natural Science and Technology, Gifu University, Yanagido 1-1, Gifu 501-1193, Japan.

<sup>2</sup> Department of Chemistry and Biomolecular Science, Faculty of Engineering, Gifu University, Yanagido 1-1, Gifu 501-1193, Japan.

<sup>3</sup> National Institute of Advanced Industrial Science and Technology (AIST), 4-2-1 Nigatake, Sendai 983-8551, Japan.

\*Corresponding authors

K. Komura, komura.kenichi.x4@f.gifu-u.ac.jp

T. Ikeda, takuji-ikeda@aist.go.jp

### EXPERIMENTAL

#### Characterizations

Powder X-ray diffraction (XRD) diagrams (Shimadzu XRD-6000) were measured using Cu K $\alpha$  radiation ( $\lambda = 1.5418 \text{ \AA}$ ). Elemental analyses were performed using X-ray fluorescence spectroscopy (XRF; Bruker S8 TIGER). Nitrogen adsorption isotherm measurements were performed using an absorption analyzer (Bel Japan Belsorp 28SA), and ammonia temperature-programmed desorption (NH<sub>3</sub>-TPD) experiments were conducted on a TPD-66 apparatus (Bel Japan): the sample was evacuated at 400°C for 1 h, and ammonia was adsorbed at 100°C followed by further evacuation for 1 h. Then, the sample was heated from 100°C to 710°C at a temperature increase of 10°C/min in a helium stream. Thermogravimetric (TGA) and differential thermal analysis (DTA) were conducted using an apparatus (Shimadzu DTG-50) with the ramp rate at 10 °C/min under an air stream. The crystal size and morphology were measured using a field-emission scanning electron microscopy (FE-SEM) (S-4800; Hitachi High-Technologies, Japan).

Local structures around <sup>1</sup>H, <sup>13</sup>C, <sup>27</sup>Al, and <sup>31</sup>P nuclei in as-synthesized GAM-7 were investigated by the solid-state magic angle spinning (MAS) nuclear magnetic resonance (NMR) using an AVANCEIII 400WB spectrometer (Bruker Biospin K.K., Japan). <sup>31</sup>P dipolar decoupling (DD) MAS NMR, {<sup>1</sup>H}-<sup>31</sup>P cross-polarization (CP)/MAS NMR, <sup>27</sup>Al direct-excitation (DE) MAS NMR, {<sup>1</sup>H}-<sup>27</sup>Al CP/MAS NMR and <sup>1</sup>H DEMAS spectra were recorded using a 4.0 mm VT-MAS probe with a rotor spinning rate of 14 kHz. {<sup>1</sup>H}-<sup>13</sup>C CP/MAS spectrum was collected with a spinning rate of 6 kHz for <sup>13</sup>C. <sup>27</sup>Al 3QMAS NMR spectrum with z-filter was also measured using a 3.2 mm triple channel VT-MAS probe with {<sup>1</sup>H} decoupling and spinning rate of 24 kHz. {<sup>27</sup>Al}-<sup>31</sup>P 3QHETCOR spectrum with a double

decoupling ( $^1\text{H}$  and  $^{27}\text{Al}$ ) sequence was also measured with a spinning rate of 15 kHz.  $(\text{NH}_4)_2\text{HPO}_4$  powder, 1.0 M  $\text{AlCl}_3$  aqueous solution, and adamantane powder were used as chemical shift secondary reference materials for  $^{31}\text{P}$ ,  $^{27}\text{Al}$ , and  $^{13}\text{C}$  nuclei, respectively.

### Preparation of $\text{AlPO}_4\text{-5}$

The typical synthetic procedure of  $\text{AlPO}_4\text{-5}$  was as follows. To a mixture of  $\text{H}_3\text{PO}_4$  (19.5 g, 85wt% in water),  $\text{Al}(\text{O}^i\text{Pr})_3$  (26.6 g) and triethylamine (10.5 g) in distilled water (32.2 g) was added diluted HF (0.38 g, 55 wt% in water) in distilled water (2.0 g). The resulting mixture was stirred at room temperature for 2 h and then transferred into a Teflon-lined autoclave. The hydrothermal synthesis was performed at 170 °C for 6 h under static conditions. The obtained product was filtered by suction, washed with distilled water, and dried at 90 °C overnight. Then, the calcination was performed at 600 °C (ramping rate 1 °C/min) for 6 h under airflow to yield the parent  $\text{AlPO}_4\text{-5}$ .

### Preparation of SAPO-5

The SAPO-5 was prepared according to the reported procedure. The  $\text{Al}(\text{O}^i\text{Pr})_3$  (22.1 g, 54 mmol) was added to 29.4 g of distilled  $\text{H}_2\text{O}$  at room temperature and stirred overnight. Then, a diluted aqueous  $\text{H}_3\text{PO}_4$  (85 wt%) solution (12.5 g, 54 mmol) and 13.7 g  $\text{H}_2\text{O}$ , and triethylamine (5.46 g, 54 mmol) were added at ambient temperature. The resulting mixture was then added to the prescribed amount of  $\text{Si}(\text{OEt})_4$  (TEOS) and was further stirred for an hour to obtain a gel. The hydrothermal synthesis was taken place at 180°C for 24 h under static conditions. After cooling down, the mixture was filtrated by suction, and the obtained solid was washed with distilled water, and then dried at 90 °C overnight. The as-synthesized solid was calcined under airflow at 600 °C for 6 h (ramping rate: 1°C/min) to yield SAPO-5.

### The interzeolite conversion

The *izcAP* of  $\text{AlPO}_4\text{-5}$ ; To aqueous solution of diisopropylamine (0.83 g, 8.2 mmol) in distilled water (4.1 g) was added the prescribed amount of the parent  $\text{AlPO}_4\text{-5}$  zeolite, where gel composition is adjusted as following mol ratio;  $\text{T}_2\text{O}_4 : \text{OSDA} : \text{H}_2\text{O} = 1.0 : 1.0 : 27.5$ . The resulting mixture was transferred to a Teflon-lined autoclave and stood at 170 °C for desired period. After cooling to ambient temperature, the product was filtrated, washed with distilled water, and dried.

The *izcMAP* of SAPO-5; The procedure of the *izcMAP* for  $[\text{Si}]\text{GAM-7}$  was the same as mentioned above, and the mixture of chemical composition was as follows;  $\text{T}_2\text{O}_4 : \text{OSDA} : \text{H}_2\text{O} = 1.0 : 1.0 : 27.5$ .

### Hydrothermal synthesis of GAM-7

The suspension of  $\text{Al}(\text{O}^i\text{Pr})_3$  (2.0 g, 5.0 mmol) in distilled water (5.3 g) was added an aqueous  $\text{H}_3\text{PO}_4$  solution (1.2 g, 5.0 mmol), and then, stirred for 1 h at room temperature. The resulting mixture was added a diisopropylamine (1.0 g, 10 mmol), of which gel composition was  $\text{Al}_2\text{O}_3 : \text{P}_2\text{O}_5 : \text{OSDA} : \text{H}_2\text{O} = 0.5 : 0.5 : 1.0 : 27.5$ . After stirring 1 h, the hydrogel was transferred to a Teflon-lined autoclave, and the hydrothermal synthesis was performed at 170 °C for desired period. The obtained solid was filtrated, washed with distilled water, and dried.

### Structure analysis

A high-resolution powder XRD data was collected on the Bruker D8 Advance with Vario-1

diffractometer (Bruker AXS, Japan) equipped with a primary curved monochromator Ge(111) provide Cu  $K\alpha_1$  radiation and a 1D position sensitive detector (Bruker VANTECH-1, detection solid angle  $2\theta = 6^\circ$ ). The diffractometer was operated at an output of 40 kV–50 mA at room temperature. A total measurement time was 38.25 h. A powder sample was packed into a borosilicate glass capillary tube with inner diameter of 0.5 mm.

Lattice constants and a space group were estimated by the indexing analysis using the program Conograph v2.0 [S1], yielding a monoclinic lattice constant uniquely. Observed integral intensities ( $I_{\text{obs}}$ ) of each diffraction peaks were extracted by the Le Bail method [S2] and a framework structure was solved by the direct method using the  $I_{\text{obs}}$  dataset, which are conducted by the program EXPO2014 [S3]. At this stage, GAM-7 has a layered structure was elucidated. Subsequently, a structure refinement was conducted using a preliminary framework model and several temporarily atomic sites as OSDA in the interlayer by the Rietveld method using the program RIETAN-FP v3.0 [S4]. Several constrains for bond lengths (T–O) and bond angles (O–T–O) were applied for optimization of framework geometry. A detailed molecular conformation of diisopropylamine in the interlayer was estimated by the direct space method using the program FOX 2022.1 [S5]. In this analysis, all framework atoms were fixed to the coordinates determined above, and position and conformation of diisopropylamine were optimized [S6]. Finally, the preliminary model including diisopropylamine was refined. Structural models were visualized by the program VESTA3 [S7]. An experimental and crystallographic information are summarized in **Table S4**. The final structural parameters are listed in **Table S5** as a crystallographic information file (CIF) format.

[S1] R. Oishi-Tomiyasu, *Acta Cryst.*, 2016, **A72**, 73–80.

[S2] A. Le Bail, H. Duroy, J.L. Fourquet, *Mater. Res. Bull.* 1988, **23**, 447–452.

[S3] A. Altomare, C. Cuocci, C. Giacovazzo, A. Moliterni, R. Rizzi, N. Corriero and A. Falcicchio, (2013). *J. Appl. Cryst.* 46, 1231-1235.

[S4] F. Izumi and K. Momma, *Solid State Phenom.*, 2007, **130**, 15.

[S5] V. Favre-Nicolin, R.J. Cerny, *Appl. Crystallogr.* **2002**, 35, 734–743

[S6] T. Ikeda, T. Nakaoka, K. Yamamoto, *Microporous Mesoporous Mater.*, **2019**, 284, 19–24.

[S7] K. Momma and F. Izumi, *J. Appl. Crystallogr.*, 2011, **44**, 1272.

[S8] D. Altermatt and I. D. Brown, *Acta Crystallogr.*, 1985, **B41**, 244.

[S9] <https://www.iucr.org/resources/data/data-sets/bond-valence-parameters>

## Contents

**Table S1.** Textural parameters of parent zeolites of AlPO<sub>4</sub>-5 and SAPO-5.

**Table S2.** Textural parameters of other parent zeolites in this study.

**Table S3.** Screening of the *izcAP* of AlPO<sub>4</sub>-5.

**Table S4.** Experimental conditions and crystallographic information.

**Table S5.** Crystallographic information file (CIF) of GAM-7.

**Fig. S1.** Powder XRD charts by the *izcMAP* of SAPO-5(0.20).

**Fig. S2.** Powder XRD charts by the *izcMAP* of SAPO-5(0.05).

**Fig. S3.** Powder XRD charts by the *izcAP* of AlPO<sub>4</sub>-11 (left), and FE-SEM images of AlPO<sub>4</sub>-11 (right, up) and the product after 3 days (right, down).

**Fig. S4.** Powder XRD charts by the *izcAP* of AlPO<sub>4</sub>-14 (left), and FE-SEM images of AlPO<sub>4</sub>-14 (right, up) and the product after 5 days (right, down).

**Fig. S5.** Powder XRD charts by the *izcMAP* of CoAPO-5(0.10), and FE-SEM images of CoAPO-5(0.10) (right, up) and the product after 5 days (right, down).

**Fig. S6.** Powder XRD charts by the *izcMAP* of GeAPO-5(0.10), and FE-SEM images of GeAPO-5(0.10) (right, up) and the product after 3 days (right, down).

**Fig. S7.** Powder XRD charts by the *izcMAP* of SAPO-11(0.10), and FE-SEM image of SAPO-11(0.10) (right).

**Fig. S8.** Powder XRD charts by the *izcMAP* of GeAPO-11(0.10), and FE-SEM images of GeAPO-11(0.10) (right, up) and the product after 3 days (right, down).

**Fig. S9.** FE-SEM image of GAM-7 synthesized by HTS using an aluminophosphate hydrogel.

**Fig. S10.** Powder XRD charts of the obtained product by HTS method using silico-aluminophosphate gel.

**Fig. S11.** TG-DTA chart of the GAM-7.

**Fig. S12.** Solid-state <sup>13</sup>C MAS NMR spectrum of GAM-7.

**Fig. S13.** Solid-state <sup>1</sup>H MAS NMR spectrum of GAM-7.

**Fig. S14.** Solid-state <sup>27</sup>Al MAS (a) and <sup>27</sup>Al CP/MAS NMR (b) spectra of GAM-7.

**Fig. S15.** Solid-state <sup>27</sup>Al 3QMAS NMR spectrum of GAM-7.

**Fig. S16.** Solid-state <sup>31</sup>P DDMAAS NMR (a) and <sup>31</sup>P CP/MAS NMR spectra of GAM-7.

**Fig. S17.** Solid-state {<sup>27</sup>Al}→<sup>31</sup>P 3QHETCOR NMR spectrum of GAM-7.

In the dotted area, the spectral intensity was increased by a factor of 5 to emphasize the weak peaks. The peak labels in each projected spectrum correspond to the site labels in the crystal structure model described in Table S5.

**Fig. S18.** The crystal structure of GAM-7 viewed along the *a*-axis.

**Fig. S19.** The crystal structure of GAM-7 viewed along the *b*-axis.

**Fig. S20.** The crystal structure of GAM-7 viewed along the *c*-axis.

**Fig. S21.** Observed (red crosses), calculated (light blue solid line), and difference (blue) patterns obtained by the Rietveld refinement for GAM-7. Tick marks (green) denote the peak positions of possible Bragg reflections. The inset shows magnified patterns from 28° to 110°.

**Fig. S22.** Powder XRD charts during the *izcAP* corresponding to experimental results in Figure 7.

**Table S1.** Textural parameters of parent zeolites of AlPO<sub>4</sub>-5 and SAPO-5.

parent zeolite	chemical composition <sup>a</sup>			surface area <sup>b</sup> (m <sup>2</sup> /g)	pore volume <sup>b</sup> (mL/g)
	Al <sub>2</sub> O <sub>3</sub>	P <sub>2</sub> O <sub>5</sub>	SiO <sub>2</sub>		
AlPO <sub>4</sub> -5	0.51	0.49	—	242	0.19
SAPO-5(0.20)	0.25	0.23	0.045	357	0.27
SAPO-5(0.05)	0.26	0.24	0.01	259	0.22
SAPO-5(0.01)	0.26	0.24	0.002	281	0.29

a Measured by XRF

b Estimated by N<sub>2</sub> adsorption isotherm.

**Table S2.** Textural parameters of other parent zeolites in this study.

parent zeolite	FTC <sup>a</sup>	chemical composition <sup>b</sup>			surface area <sup>c</sup> (m <sup>2</sup> /g)	pore volume <sup>c</sup> (mL/g)
		Al <sub>2</sub> O <sub>3</sub>	P <sub>2</sub> O <sub>5</sub>	TO <sub>2</sub> <sup>d</sup>		
AlPO <sub>4</sub> -11	<b>AEL</b>	0.48	0.34	—	157	0.33
AlPO <sub>4</sub> -14	<b>AFN</b>	0.41	0.41	—	199	0.15
CoAPO-5(0.10)	<b>AFI</b>	0.47	0.45	0.09	208	0.15
GeAPO-5(0.10)		0.44	0.36	0.04	113	0.25
SAPO-11(0.05)		0.43	0.39	0.02	74	0.22
SAO-11(0.01)	<b>AEL</b>	0.43	0.37	0.005	58	0.24
GeAPO-11(0.10)		0.43	0.38	0.02	131	0.28

a Framework type code

b Estimated by XRF

c Estimated by N<sub>2</sub> adsorption analysis

d Amount of incorporated heteroatom

**Table S3.** Screening of the *izcAP* of AlPO<sub>4</sub>-5.<sup>a</sup>

entry	OSDA <sup>b</sup>	H <sub>2</sub> O <sup>c</sup>	time (d)	product <sup>d</sup>
1			3	AlPO <sub>4</sub> -5 + GAM-7
2	0.30	27.5	5	AlPO <sub>4</sub> -5 + tridymite
3			7	AlPO <sub>4</sub> -5 + tridymite
4			3	AlPO <sub>4</sub> -5 + tridymite
5	0.30	21.0	5	tridymite
6			7	tridymite
7			3	AlPO <sub>4</sub> -5 + GAM-7 + tridymite
8	0.30	13.5	5	AlPO <sub>4</sub> -5 + GAM-7 + tridymite
9			7	GAM-7 + tridymite
10 <sup>e</sup>	0.30	13.5	5	AlPO <sub>4</sub> -11 + tridymite
11e			7	AlPO <sub>4</sub> -11 + tridymite
12			3	GAM-7
13	0.60	27.5	5	GAM-7
14			7	GAM-7
15	1.0	27.5	2	GAM-7
16			4	GAM-7
17 <sup>f</sup>			3	AlPO <sub>4</sub> -5 + unknown
18f	0.80	27.5	5	AlPO <sub>4</sub> -11 + unknown
19f			7	AlPO <sub>4</sub> -11 + unknown

a The *izcAP* was performed using AlPO<sub>4</sub>-5 as the parent and diisopropylamine as the OSDA at 170 °C.

b The molar ratio of OSDA/T<sub>2</sub>O<sub>4</sub>.

c The molar ratio of H<sub>2</sub>O/T<sub>2</sub>O<sub>4</sub>.

d Assigned by powder XRD.

e HF (HF/T<sub>2</sub>O<sub>4</sub> = 0.05) was added.

f H<sub>3</sub>PO<sub>4</sub> (H<sub>3</sub>PO<sub>4</sub>/T<sub>2</sub>O<sub>4</sub> = 0.23) was added.

**Table S4.** Experimental conditions and crystallographic information for GAM-7.

Compound name	GAM-7
Estimated chemical composition	$[(C_6H_{15}N)_{3.67}] \cdot [Al_{16}P_{12}O_{44}(OH)_{20}]$
Space group	$P2_1/c$
$a / \text{nm}$	1.367980(11)
$b / \text{nm}$	1.420480(12)
$c / \text{nm}$	0.999269(8)
$\beta / ^\circ$	100.0990(9)
Unit-cell volume, $V / \text{nm}^3$	1.91168(3)
$2\theta$ range / $^\circ$	4.0–110.1
Step size ( $2\theta$ ) / $^\circ$	0.016346
Profile range in FWHM	12
Number of observations	6502
Number of contributing reflections	2406
Number of refined structural parameters	158
Number of constraints	167
$R$ -factors, goodness-of-fit indicator obtained by Rietveld analysis.	
$R_{\text{wp}}$	0.026
$R_{\text{p}}$	0.021
$R_{\text{F}}$	0.014
$R_{\text{Bragg}}$	0.015
$R_{\text{exp}}$	0.015
$S$	1.797
$\chi^2$	3.22

**Table S5.** Crystallographic information file (CIF) of GAM-7.

```

=====
# CRYSTAL DATA
#-----
data_VESTA_phase_1

_chemical_name_common          'GAM-7'
_cell_length_a                 13.67980(11)
_cell_length_b                 14.20480(12)
_cell_length_c                 9.99269(8)
_cell_angle_alpha              90.000000
_cell_angle_beta               100.0990(10)
_cell_angle_gamma              90.000000
_cell_volume                   1911.682503
_space_group_name_H-M_alt      'P 21/c'
_space_group_IT_number         14

loop_
_space_group_symop_operation_xyz
  'x, y, z'
  '-x, -y, -z'
  '-x, y+1/2, -z+1/2'
  'x, -y+1/2, z+1/2'

loop_
_atom_site_label
_atom_site_fract_x
_atom_site_fract_y
_atom_site_fract_z
_atom_site_occupancy
_atom_site_symmetry_multiplicity
_atom_site_Wyckoff_symbol
_atom_site_adp_type
_atom_site_U_iso_or_equiv
_atom_site_type_symbol
Al1      0.2228(4)  0.2110(4)  0.4334(6)  1      4 e Uiso  0.0171(3)  Al
Al2      0.5672(5)  0.3548(4)  0.0155(6)  1      4 e Uiso  0.0171(3)  Al
Al3      0.3787(5)  0.1123(4)  0.0612(6)  1      4 e Uiso  0.0171(3)  Al
Al4      0.5627(4)  0.0139(4)  0.1361(5)  1      4 e Uiso  0.0171(3)  Al
P1       0.3660(4)  0.4488(4)  0.0534(5)  1      4 e Uiso  0.0171(3)  P
P2       0.1632(5)  0.1576(4)  0.1383(5)  1      4 e Uiso  0.0171(3)  P
P3       0.5554(4)  0.2164(4)  0.2322(5)  1      4 e Uiso  0.0171(3)  P
O1       0.6424(8)  0.4481(7)  -0.003(1)  1      4 e Uiso  0.0210(8)  O
O2       0.3835(8)  0.4427(7)  0.216(1)   1      4 e Uiso  0.0210(8)  O
O3       0.2702(8)  0.1043(8)  0.497(1)   1      4 e Uiso  0.0210(8)  O
O4       0.4488(8)  0.3992(7)  -0.005(1)  1      4 e Uiso  0.0210(8)  O
O5       0.5669(8)  0.2318(7)  0.390(1)   1      4 e Uiso  0.0210(8)  O
O6       0.5991(8)  0.3043(8)  0.172(1)   1      4 e Uiso  0.0210(8)  O
O7       0.3293(9)  0.4894(9)  0.450(1)   1      4 e Uiso  0.0210(8)  O
O8       0.2753(9)  0.1182(7)  0.150(1)   1      4 e Uiso  0.0210(8)  O
O9       0.498(1)   0.4061(8)  0.474(1)   1      4 e Uiso  0.0210(8)  O
O10      0.3223(8)  0.2937(8)  0.422(1)   1      4 e Uiso  0.0210(8)  O
O11      0.4419(8)  0.0269(8)  0.193(1)   1      4 e Uiso  0.0210(8)  O
O12      0.4450(7)  0.2116(8)  0.171(1)   1      4 e Uiso  0.0210(8)  O
O13      0.6100(8)  0.1254(8)  0.208(1)   1      4 e Uiso  0.0210(8)  O

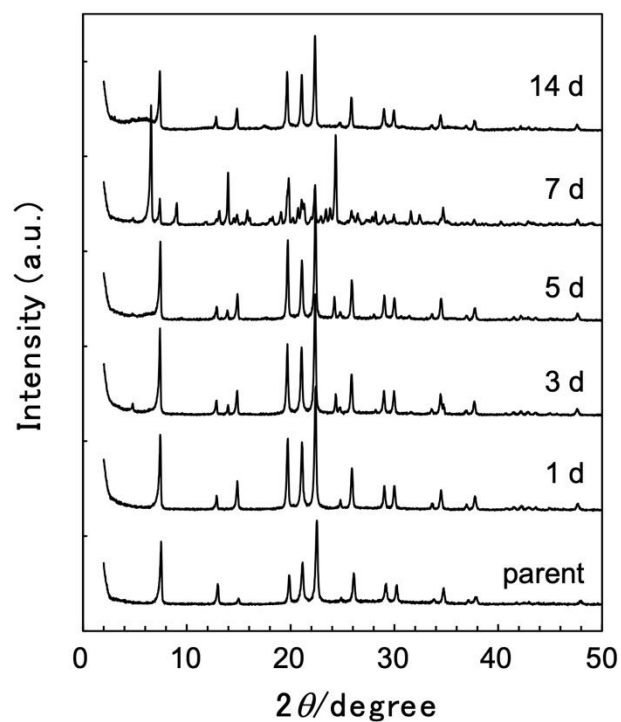
```

Table S5. Continued.

O14	0.1434(8)	0.2432(7)	0.038(1)	1	4 e Uiso	0.0210(8)	O
O15	0.1509(8)	0.1954(7)	0.277(1)	1	4 e Uiso	0.0210(8)	O
O16	0.0823(9)	0.0817(9)	0.088(1)	1	4 e Uiso	0.0210(8)	O
C1	0.858(2)	0.160(2)	0.833(3)	0.924(6)	4 e Uiso	0.035(3)	C
N2	0.947(1)	0.098(1)	0.842(2)	0.924(6)	4 e Uiso	0.035(3)	N
C3	0.814(2)	0.144(2)	0.958(3)	0.924(6)	4 e Uiso	0.035(3)	C
C4	0.892(2)	0.260(2)	0.835(2)	0.924(6)	4 e Uiso	0.035(3)	C
C5	0.995(2)	0.107(2)	0.719(3)	0.924(6)	4 e Uiso	0.035(3)	C
C6	1.083(2)	0.044(2)	0.735(2)	0.924(6)	4 e Uiso	0.035(3)	C
C7	0.921(2)	0.071(2)	0.602(3)	0.924(6)	4 e Uiso	0.035(3)	C
H8	0.81(1)	0.14(1)	0.74(2)	0.924(6)	4 e Uiso	0.035(3)	H
H9	0.93(1)	0.03(1)	0.85(2)	0.924(6)	4 e Uiso	0.035(3)	H
H10	0.86(1)	0.17(1)	1.05(2)	0.924(6)	4 e Uiso	0.035(3)	H
H11	0.75(1)	0.18(1)	0.94(2)	0.924(6)	4 e Uiso	0.035(3)	H
H12	0.80(1)	0.07(1)	0.97(2)	0.924(6)	4 e Uiso	0.035(3)	H
H13	0.86(1)	0.29(1)	0.73(2)	0.924(6)	4 e Uiso	0.035(3)	H
H14	0.87(1)	0.30(1)	0.92(2)	0.924(6)	4 e Uiso	0.035(3)	H
H15	0.97(1)	0.26(1)	0.84(2)	0.924(6)	4 e Uiso	0.035(3)	H
H16	1.01(1)	0.18(1)	0.71(2)	0.924(6)	4 e Uiso	0.035(3)	H
H17	1.10(1)	0.01(1)	0.83(1)	0.924(6)	4 e Uiso	0.035(3)	H
H18	1.07(1)	-0.01(1)	0.66(2)	0.924(6)	4 e Uiso	0.035(3)	H
H19	1.14(1)	0.09(1)	0.71(2)	0.924(6)	4 e Uiso	0.035(3)	H
H20	0.91(1)	0.00(1)	0.63(2)	0.924(6)	4 e Uiso	0.035(3)	H
H21	0.85(1)	0.11(1)	0.60(2)	0.924(6)	4 e Uiso	0.035(3)	H
H22	0.95(1)	0.08(1)	0.51(2)	0.924(6)	4 e Uiso	0.035(3)	H
Hm1	0.11(1)	0.02(1)	0.09(2)	1	4 e Uiso	0.0210(8)	H
Hm2	0.32(1)	0.54(1)	0.51(1)	1	4 e Uiso	0.0210(8)	H
Hm3	0.41(1)	-0.036(9)	0.20(1)	1	4 e Uiso	0.0210(8)	H
Hm4	0.52(1)	0.344(9)	0.44(1)	1	4 e Uiso	0.0210(8)	H
Hm5	0.37(1)	0.28(1)	0.36(1)	1	4 e Uiso	0.0210(8)	H

#=====

=====



**Fig. S1.** Powder XRD charts of the product by *izc*MAP of SAPO-5(0.20) for different times.

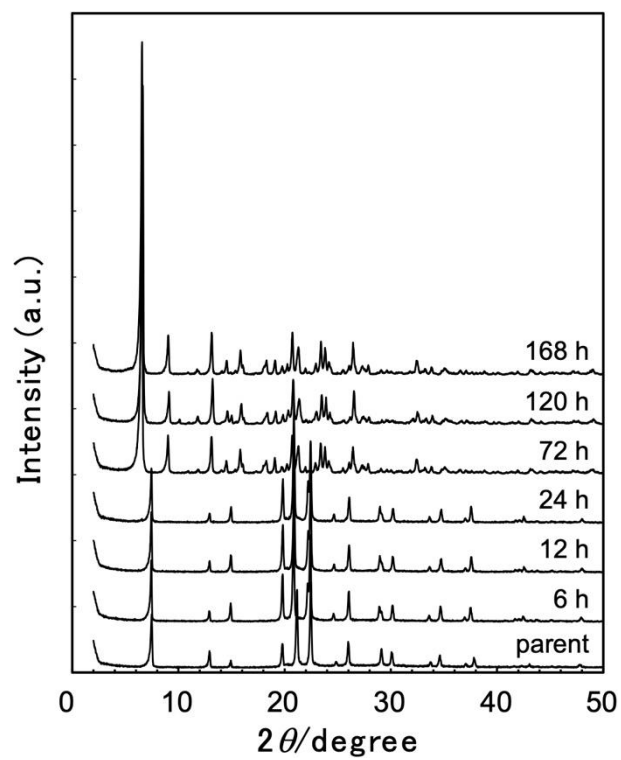


**Fig. S2.** Powder XRD charts of the product by *izc*MAP of SAPO-5(0.05) for different times.

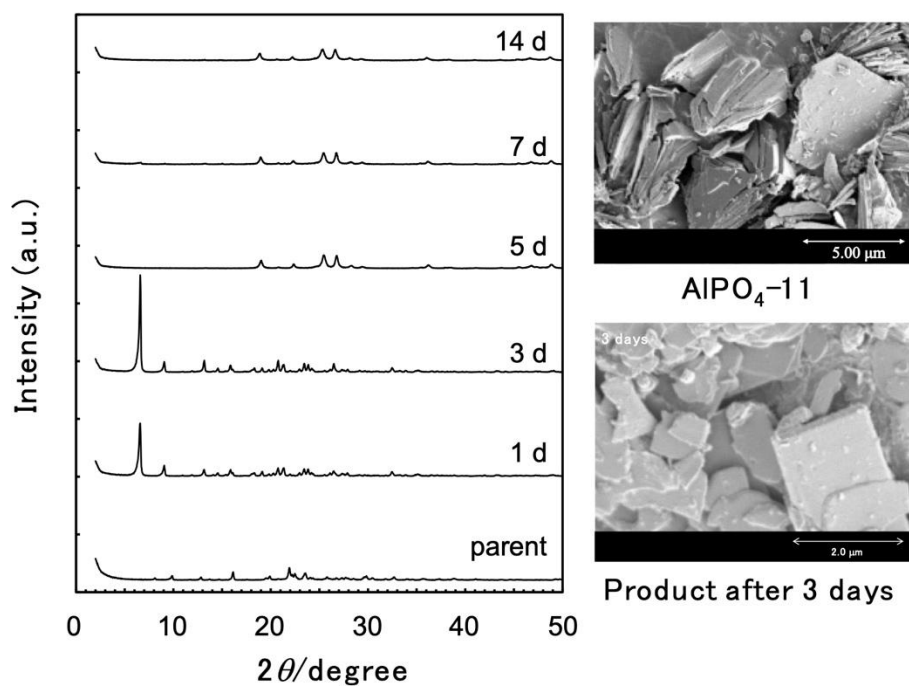


**Fig. S3.** Powder XRD charts by the *izcAP* of  $\text{AlPO}_4\text{-11}$  (left), and FE-SEM images of  $\text{AlPO}_4\text{-11}$  (right, up) and the product after 3 days (right, down).

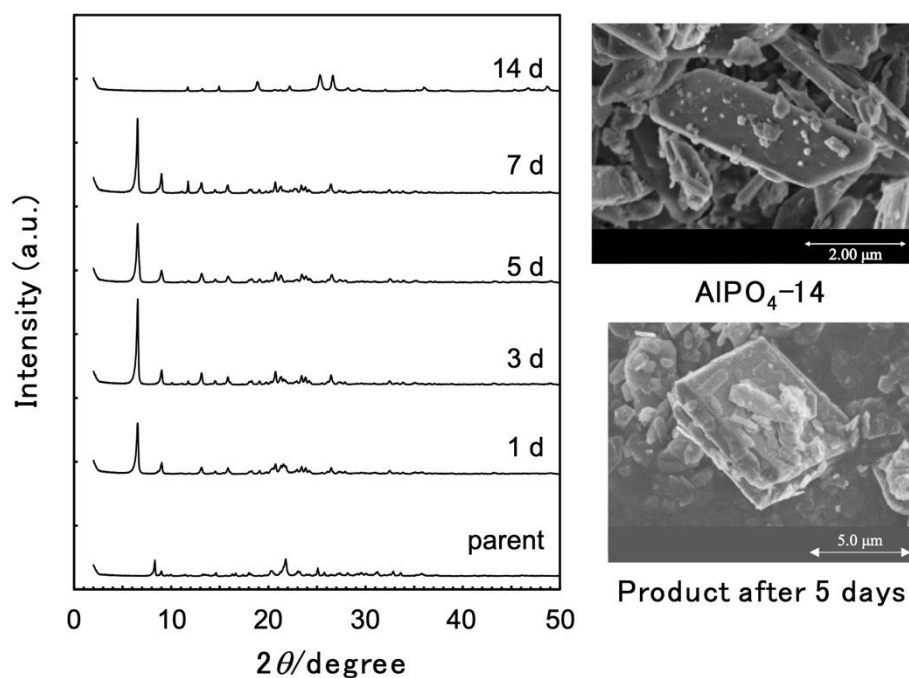


**Fig. S4.** Powder XRD charts by the *izcAP* of  $\text{AlPO}_4\text{-14}$  (left), and FE-SEM images of  $\text{AlPO}_4\text{-14}$  (right, up) and the product after 5 days (right, down).

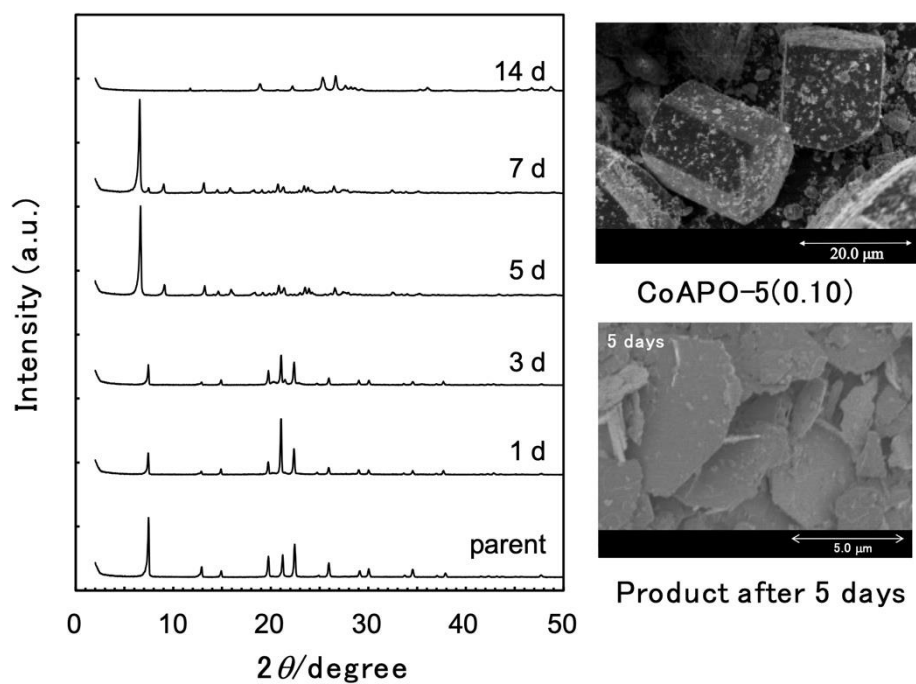


**Fig. S5.** Powder XRD charts by the *izcMAP* of CoAPO-5(0.10), and FE-SEM images of CoAPO-5(0.10) (right, up) and the product after 5 days (right, down).

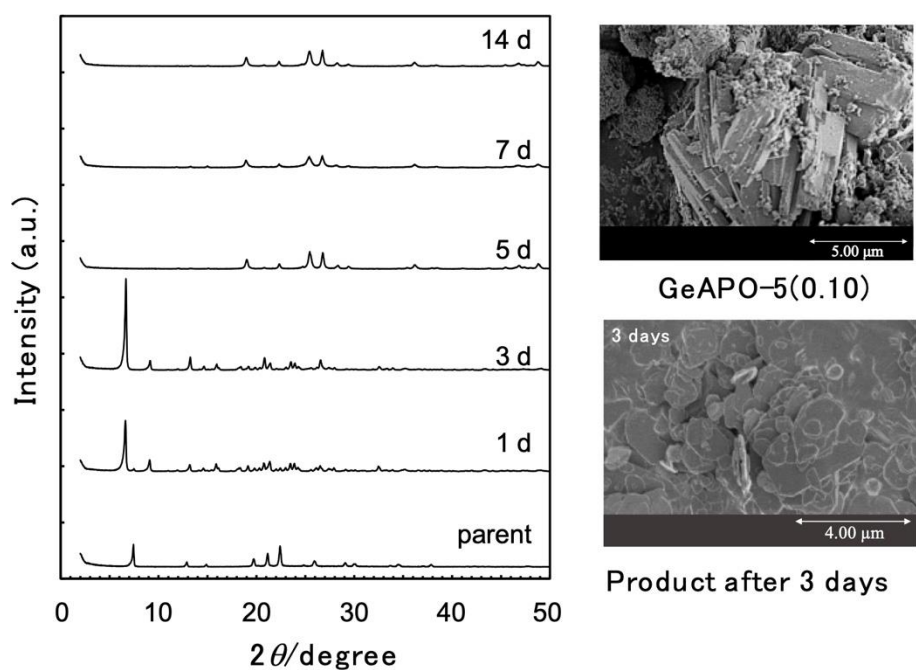


**Fig. S6.** Powder XRD charts by the *izcMAP* of GeAPO-5(0.10), and FE-SEM images of GeAPO-5(0.10) (right, up) and the product after 3 days (right, down).

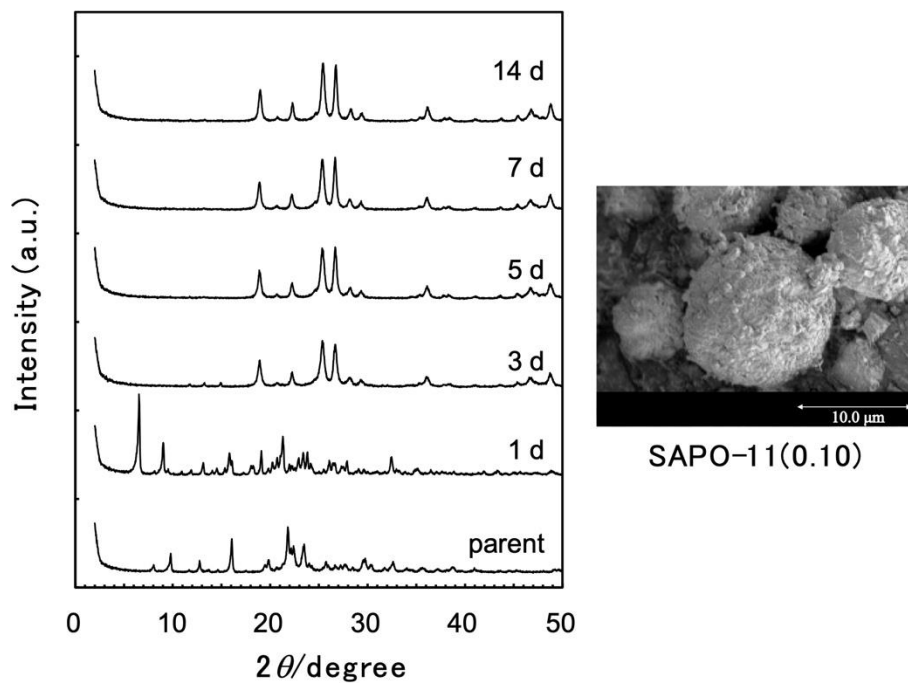


**Fig. S7.** Powder XRD charts by the *izc*MAP of SAPO-11(0.10), and FE-SEM image of SAPO-11(0.10) (right).

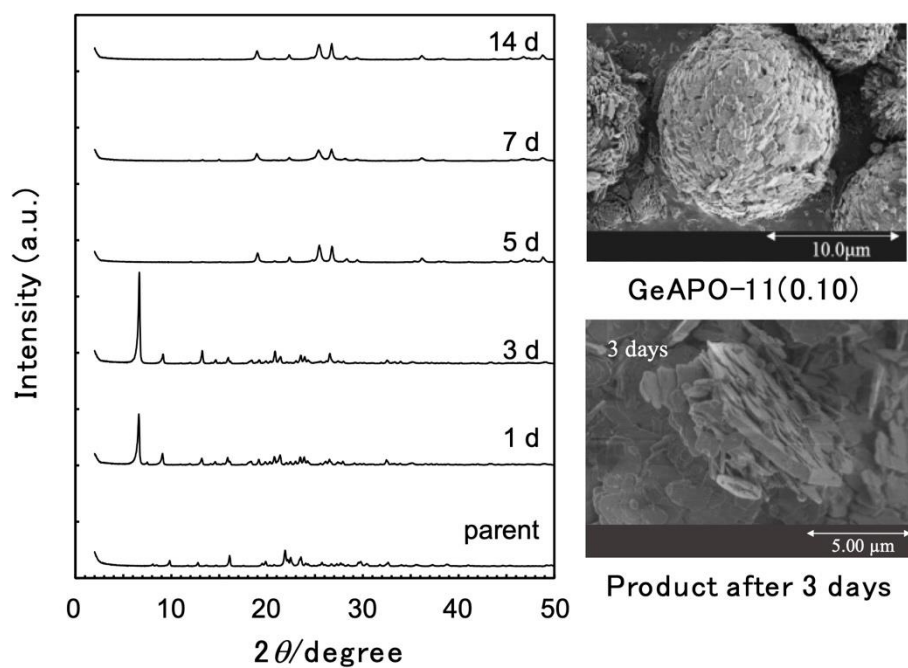


**Fig. S8.** Powder XRD charts by the *izc*MAP of GeAPO-11(0.10), and FE-SEM images of GeAPO-11(0.10) (right, up) and the product after 3 days (right, down).

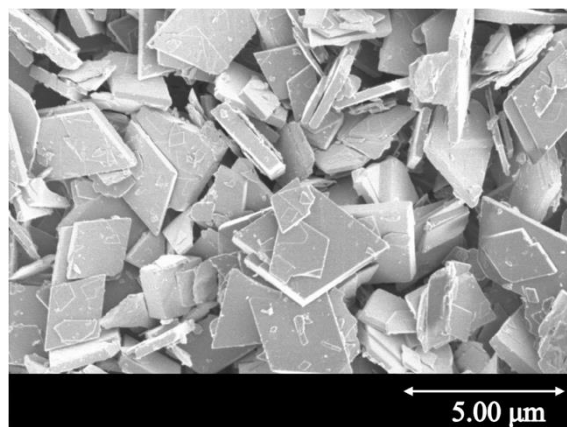


**Fig. S9.** FE-SEM image of GAM-7 synthesized by HTS method.

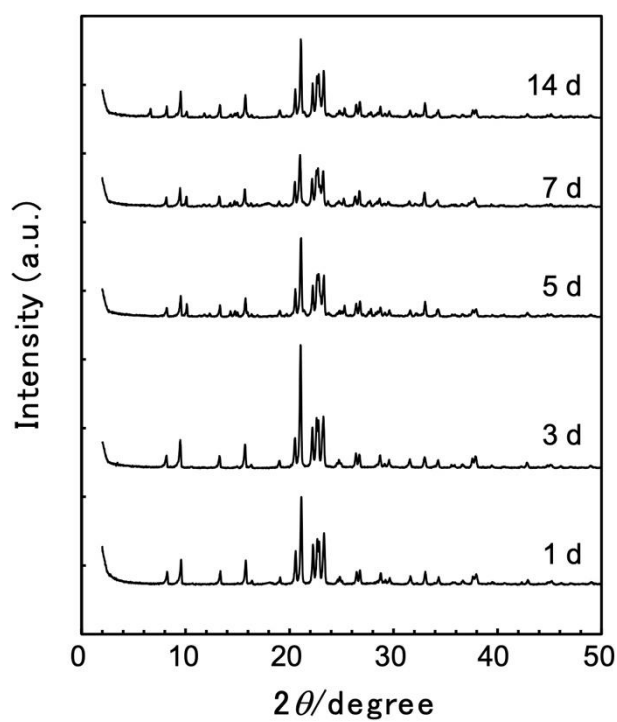


**Fig. S10.** Powder XRD charts of the obtained product by HTS method using silico-aluminophosphate gel.

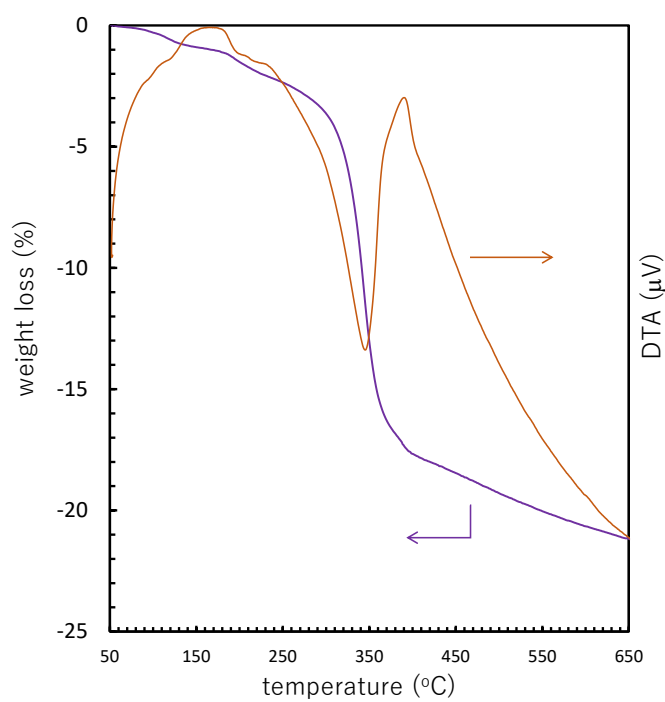


**Fig. S11.** TG-DTA chart of GAM-7.

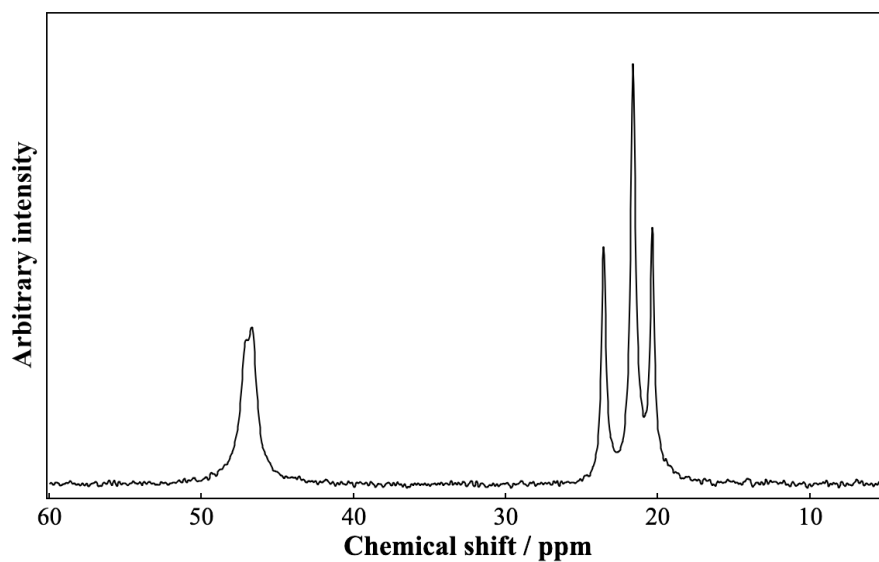


**Fig. S12.** Solid-state <sup>13</sup>C CP/MAS NMR spectrum of GAM-7.

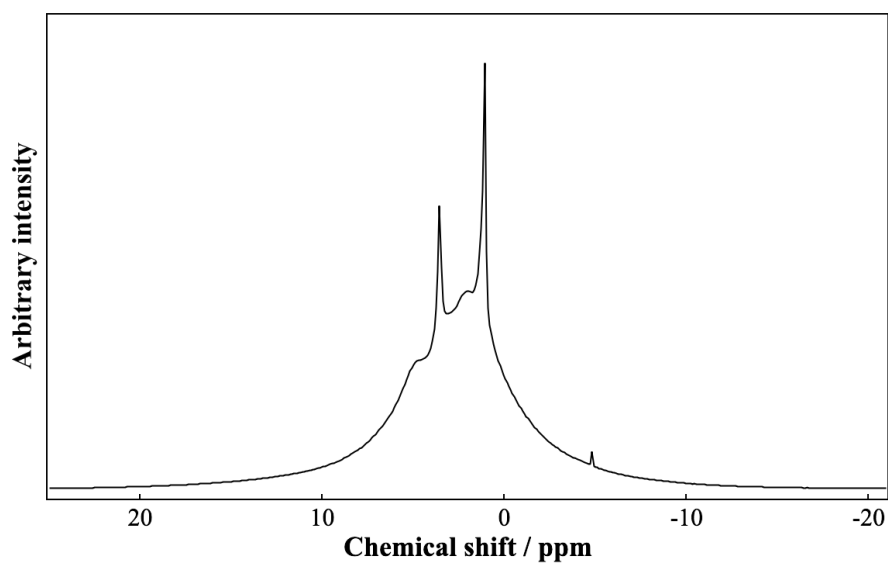


**Fig. S13.** Solid-state  $^1\text{H}$  DEMAS NMR spectrum of GAM-7.

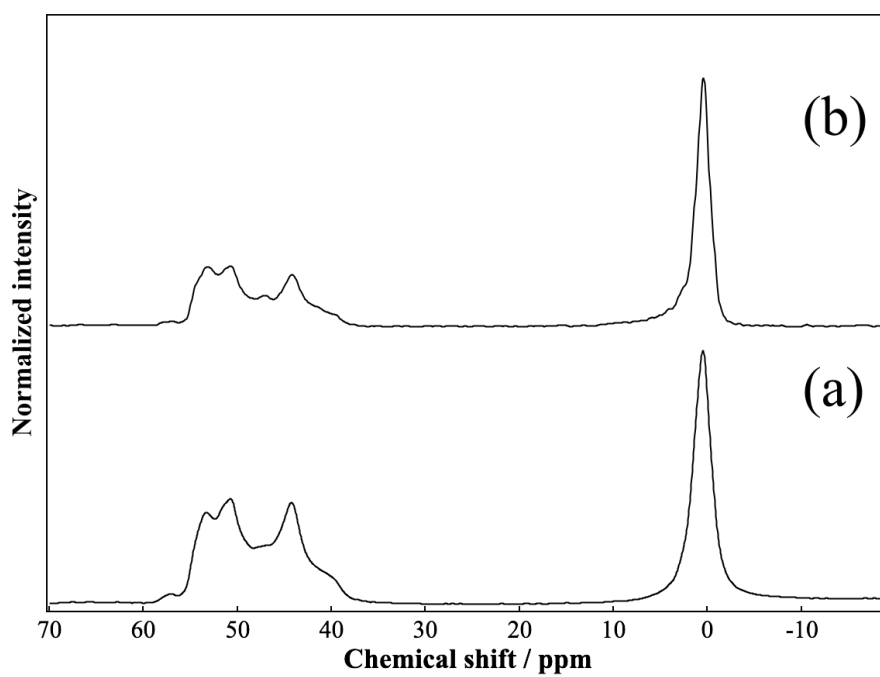


**Fig. S14.** Solid-state  $^{27}\text{Al}$  DEMAS (a) and  $^{27}\text{Al}$  CP/MAS NMR (b) spectra of GAM-7.

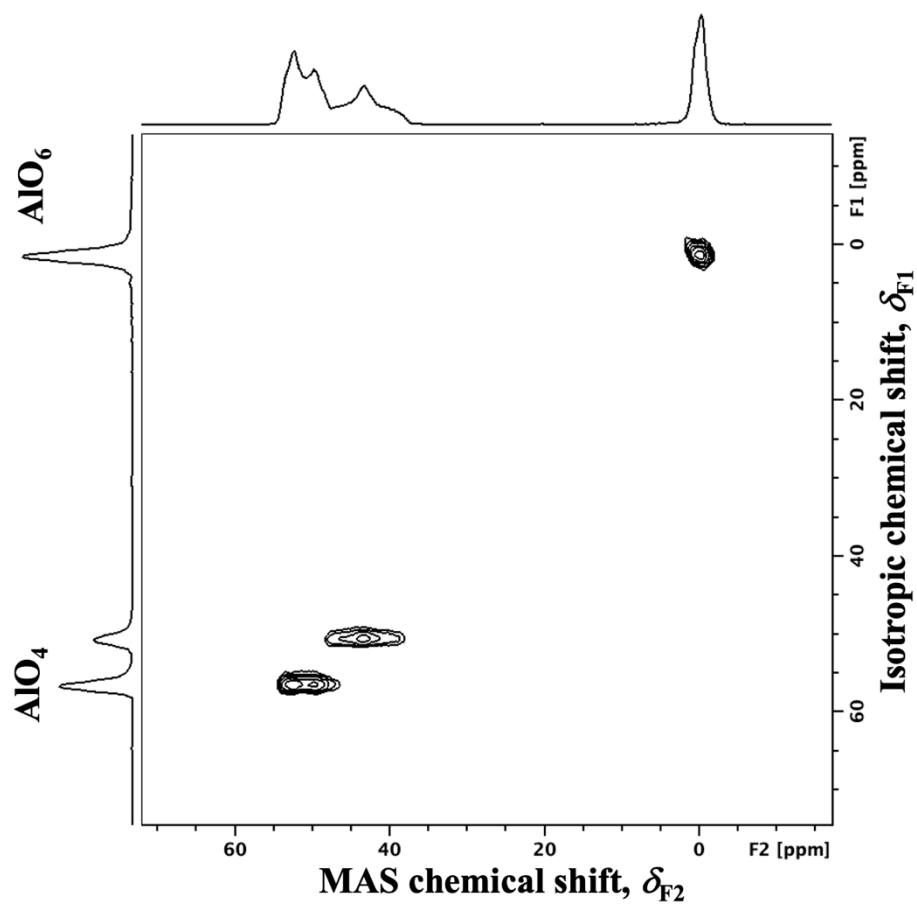


Fig. S15. Solid-state  $^{27}\text{Al}$  3QMAS NMR spectrum of GAM-7.

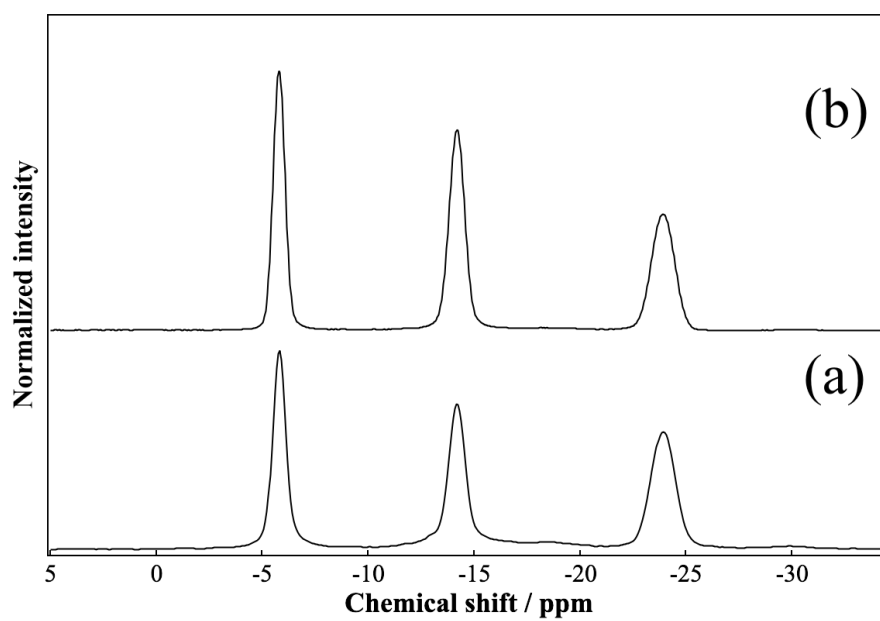
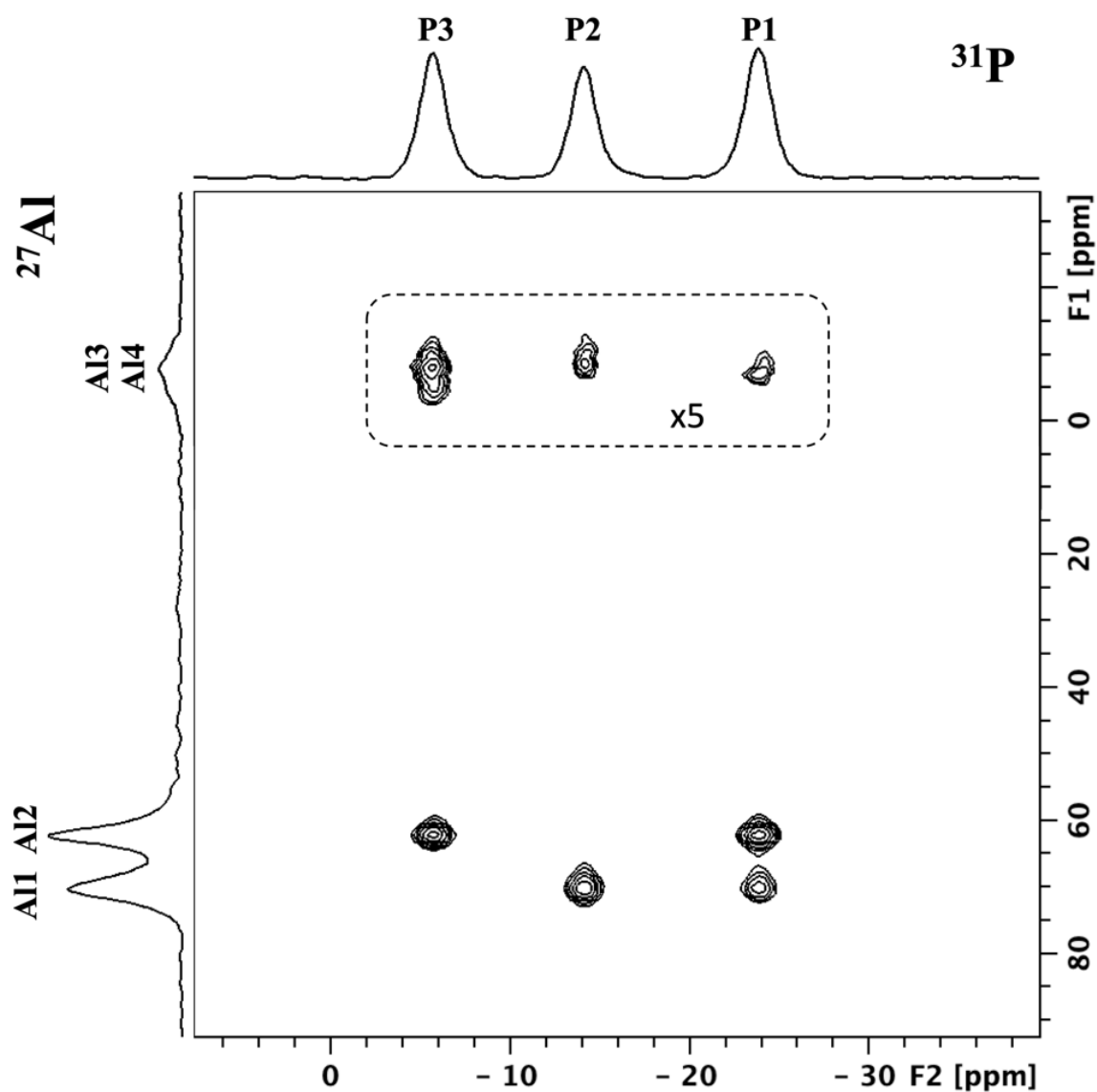


Fig. S16. Solid-state  $^{31}\text{P}$  DDMAAS NMR (a) and  $^{31}\text{P}$  CP/MAS NMR spectra of GAM-7.



**Fig. S17.** Solid-state  $\{^{27}\text{Al}\} \rightarrow ^{31}\text{P}$  3QHETCOR NMR spectrum of GAM-7. In the dotted area, the spectral intensity was increased by a factor of 5 to emphasize the weak peaks. The peak labels in each projected spectrum correspond to the site labels in the crystal structure model described in Table S5.

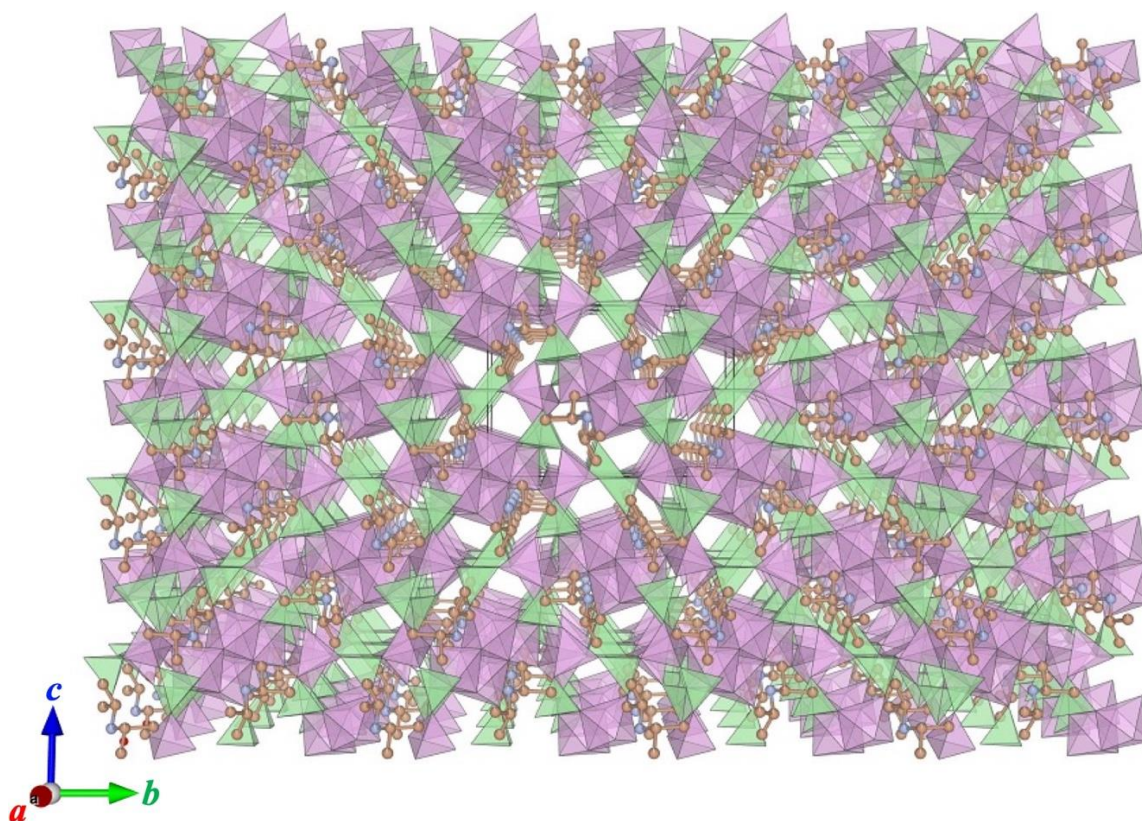


Fig. S18. The crystal structure of GAM-7 viewed along the  $a$ -axis.

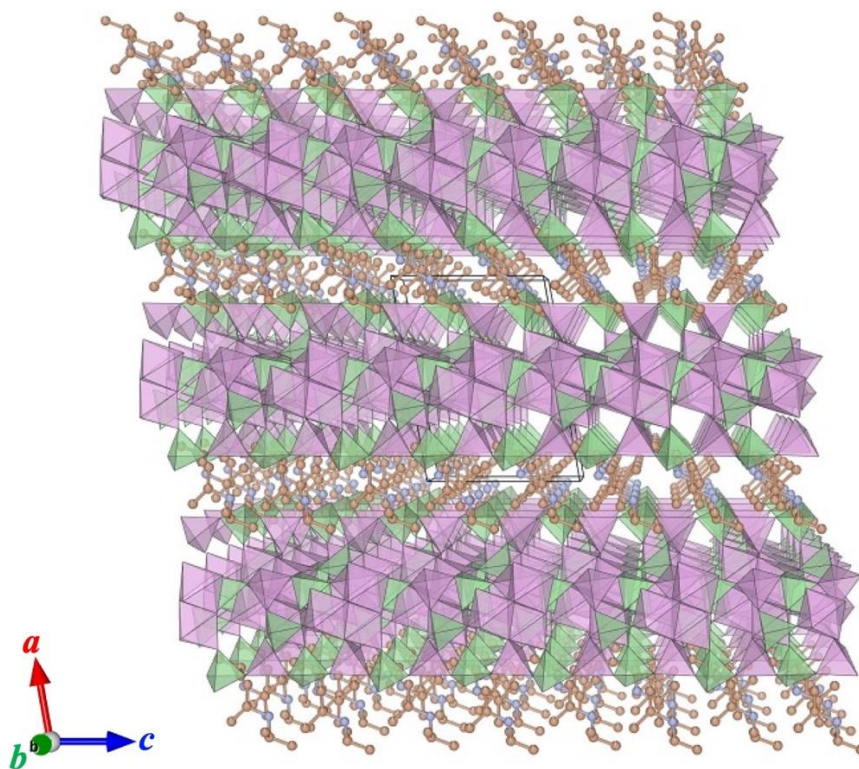
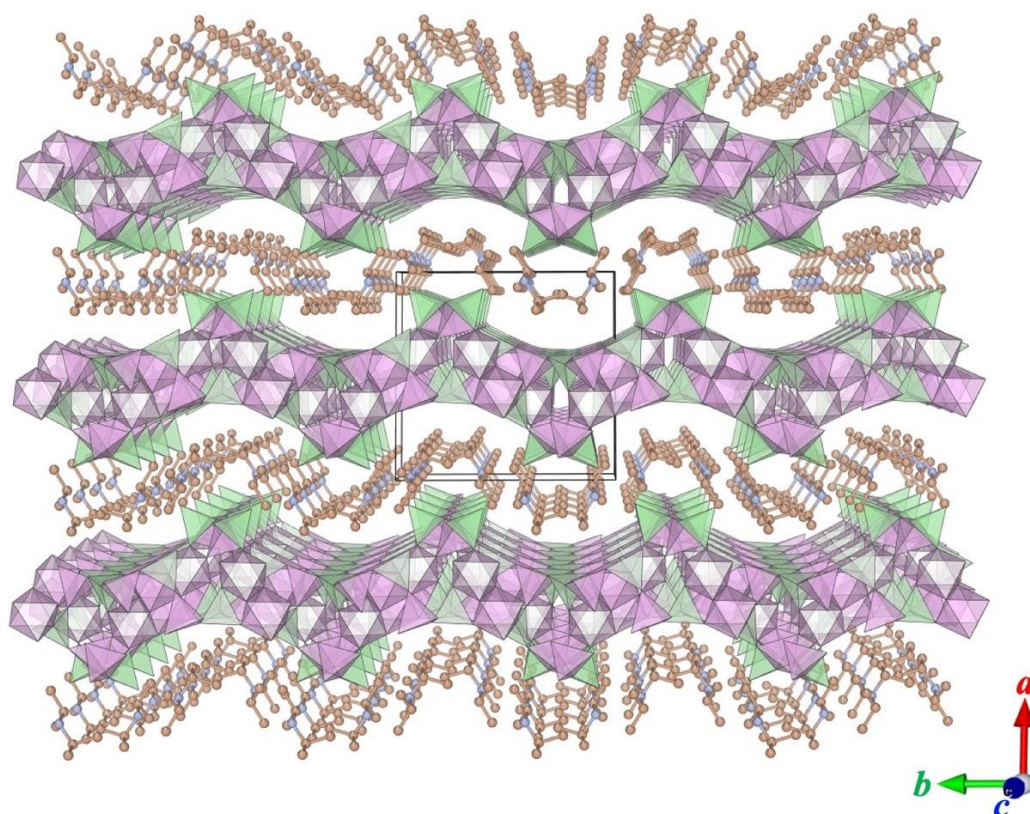
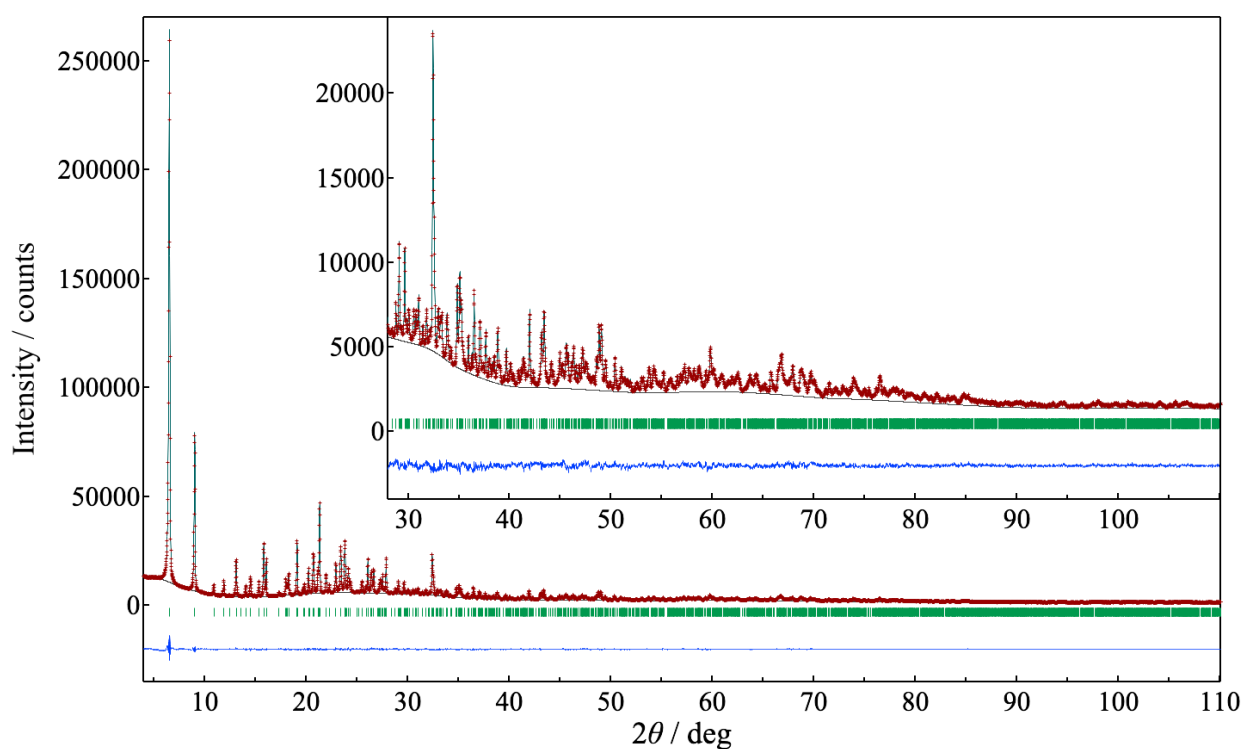


Fig. S19. The crystal structure of GAM-7 viewed along the  $b$ -axis.



**Fig. S20.** The crystal structure of GAM-7 viewed along the  $c$ -axis.



**Fig. S21.** Observed (red crosses), calculated (light blue solid line), and difference (blue) patterns obtained by the Rietveld refinement for GAM-7. Tick marks (green) denote the peak positions of possible Bragg reflections. The inset shows magnified patterns from  $28^\circ$  to  $110^\circ$ .

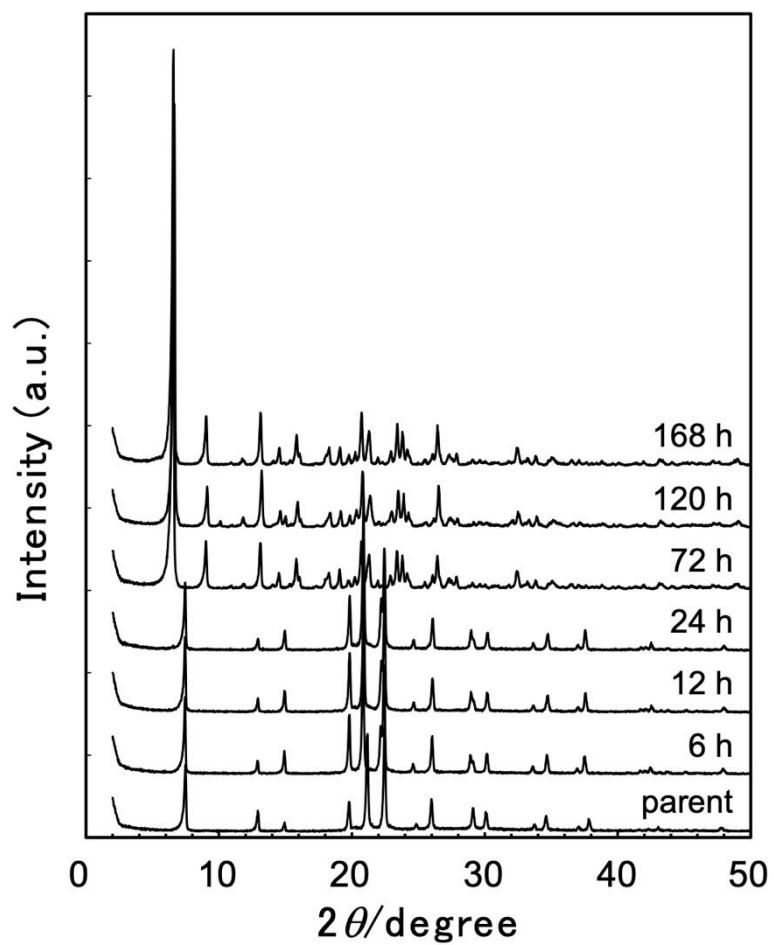


**Fig. S22.** Powder XRD charts during the *izcAP* corresponding to experimental results in Figure 5.